

# Electromagnetic bubble generation by half-cycle pulses

A. E. Kaplan, S. F. Straub,\* and P. L. Shkolnikov

Department of Electrical and Computer Engineering, The Johns Hopkins University, Baltimore, Maryland 21218

Received October 4, 1996

Electromagnetic (EM) bubbles (EMB's), unipolar, super-short, and intense nonoscillating solitary pulses of EM radiation, can be generated in a gas of nonlinear atoms by available half-cycle pulses (HCP's). We investigate how EMB's characteristics (amplitude, length, formation distance, and total number) are controlled by the amplitude and length of originating HCP's. We also predict shocklike wave fronts in the multibubble regime. © 1997 Optical Society of America

Optics usually operates with almost-harmonic oscillations with an envelope much longer than a single cycle of the oscillations. However, recent developments in time-domain spectroscopy<sup>1</sup> of dielectrics, semiconductors and flames,<sup>2</sup> transient chemical processes,<sup>3</sup> new principles of imaging,<sup>4</sup> and photoionization of atoms,<sup>5</sup> call for short and intense electromagnetic (EM) pulses of a nonoscillating nature, i.e., almost unipolar half-cycle pulses (HCP's). The spectra of currently available HCP's generated in semiconductors by optical rectification reach into the terahertz domain; these HCP's are 400–500 fs long, with a peak field of 150–200 kV/cm. Recently,<sup>6,7</sup> we proposed two new, different principles for generating much shorter (as short as 0.1 fs = 10<sup>-16</sup> s) and stronger (up to ~10<sup>16</sup> W/cm<sup>2</sup>) pulses. One of these principles is based on stimulated cascade Raman scattering<sup>6</sup> and would result in the generation of an almost-periodic train of powerful subfemtosecond pulses, while another one is based on the generation of powerful EM bubbles<sup>7</sup> (EMB's), which are unipolar EM solitons propagating in a gas of two-level<sup>7,8</sup> or classically nonlinear atoms. The latter effect would allow one to generate a single EMB or an EMB train (in which EMB's propagate with different velocities and can easily be separated into individual pulses).

One of the avenues of EMB generation is to use available HCP's to launch much shorter EMB's in a nonlinear medium. For experiments and applications one needs to know how the properties of EMB's are controlled by an incident HCP. In this Letter we answer a few important questions: Given the amplitude  $E_0$  and length  $t_0$  of an incident HCP, (1) what is leading EMB's amplitude  $E_{\text{EMB}}$  and (2) length  $t_{\text{EMB}}$ , (3) how many EMB's (per HCP) can be generated, (4) what are their amplitudes and lengths, and (5) what is the formation distance  $z_{\text{EMB}}$  at which the first EMB appears? In general, these questions cannot be answered analytically; however, our numerical and analytical efforts allowed us to obtain remarkably simple results, qualitatively summarized as follows:  $E_{\text{EMB}}$  is proportional to (and larger than)  $E_0$  for an incident HCP, and  $t_{\text{EMB}} \propto E_{\text{EMB}}^{-1}$ ; the number of EMB's is proportional to the area of the incident HCP, and  $z_{\text{EMB}} \propto E_0^{-b}$ , where  $2 \leq b \leq 3$ . We show that when many EMB's are generated, they evolve into a shocklike wave front. The good news is that very short EMB's can be generated by a much longer HCP with a large enough amplitude.

We consider here a linearly polarized wave with the electric field,  $\mathbf{E} = \hat{e}_x E(t, z)$ , propagating in the  $z$  axis in either a two-level system (TLS) characterized by the dipole moment  $\mathbf{d}$  and the resonant frequency  $\omega_0$  of its constitutive atoms and their density number  $N$  (polarization density is  $\mathbf{P} = N\mathbf{d}p$ , where  $p$  is polarization per atom) or a gas of anharmonic classical oscillators (atoms). For TLS, we use the Bloch equations, with no rotating wave approximation:

$$\dot{\eta} = -f\dot{p}, \quad \ddot{p} + p = f\eta, \quad (1)$$

where  $\tilde{\tau} = t\omega_0$ , the overdot designates  $\partial/\partial\tilde{\tau}$ ,  $f = 2\mathbf{d}\mathbf{E}/\hbar\omega_0$  is a dimensionless field, and  $\eta$  is the population difference per atom. Relaxation is not included in Eqs. (1) since all the pulses are much shorter than TLS relaxation times. The TLS approximation is valid if the instantaneous Rabi frequency is relatively small,  $\mathbf{d}\mathbf{E}/\hbar\omega_0 = f/2 \ll 1$ , which is the case throughout this Letter.<sup>9</sup> Indeed, in noble gasses,  $\hbar\omega_0 \sim 8\text{--}20$  eV, so that even with the still unachievable value  $E = 2$  MV/cm (see below),  $f/2 \sim 10^{-2}$ . In the opposite limit,  $f \gg 1$ , an atom can be modeled by a classical anharmonic oscillator with an ionization potential,  $U(p)$ , enabling one to address over-the-barrier ionization in superstrong pulses, in particular, the formation of a shock wave (dc ionization front).<sup>7</sup> In the intermediate domain, a multilevel quantum approach has to be used. The full one-dimensional Maxwell equation is

$$\partial^2 f / \partial \tilde{\zeta}^2 - \partial^2 f / \partial \tilde{\tau}^2 = Q \partial^2 p / \partial \tilde{\tau}^2. \quad (2)$$

Here  $Q \equiv 8\pi N d^2 / \hbar \omega_0 = 4\alpha N \lambda_0 (d/e)^2$ , where  $\alpha = e^2 / \hbar c = 1/137$  and  $\tilde{\zeta} = z\omega_0/c$ . If  $Q \ll 1$  (which is the case in gasses under regular conditions), no nonlinear retroreflection is expected, and Eq. (2) can with good accuracy<sup>7,8</sup> be reduced, for example, for the wave traveling in the positive direction in the  $\tilde{\zeta}$  axis, to  $\partial f / \partial \tilde{\zeta} = \partial(f - p) / \partial \tilde{\tau}$ , where  $\zeta = \tilde{\zeta} Q \beta_{\text{cr}} / 2$  is a normalized distance,  $\tau = \tilde{\tau} - \zeta / \beta_{\text{cr}}$ , and  $\beta_{\text{cr}} = (1 + Q)^{-1/2} \approx 1 - Q/2$  is the lowest (critical) speed of the EMB's.

The full Maxwell + Bloch equations (1) and (2) have an exact solitary solution<sup>7,8</sup> propagating with some fixed velocity,  $\beta_{\text{EMB}} = v_{\text{EMB}}/c$ . This solution is found by using a universal EMB-replication relationship<sup>7</sup> between the field  $f$  and polarization  $p$ :  $f = QMp$ , where  $M = (\beta_{\text{EMB}}^2 - 1)^{-1} = \text{constant}$ , which is valid for both quantum and classical systems. The EMB for a TLS is  $f(\tau) = f_{\text{EMB}} / \cosh(2\tau/\tau_{\text{EMB}})$ , where  $f_{\text{EMB}} =$

$2(QM - 1)^{1/2}$ ,  $\tau_{\text{EMB}} = 4/f_{\text{EMB}}$  are the amplitude of EMB and its length, respectively, and  $\tau = \tilde{\tau} - \tilde{\zeta}/\beta_{\text{EMB}}$  is a retarded time. A similar exact solution for  $f$  also exists for a classical anharmonic potential,<sup>7</sup>  $V(p) = p^2/2 + a_{\text{NL}}p^4/4$ , where  $a_{\text{NL}} > 0$  is the coefficient of anharmonicity. The EMB's speed of propagation is  $\beta_{\text{EMB}} = [1 + Q/(1 + f_{\text{EMB}}^2/4)]^{-1/2}$ , or, if  $Q \ll 1$ ,

$$\beta_{\text{EMB}} \approx 1 - Q/[2(1 + f_{\text{EMB}}^2/4)]. \quad (3)$$

The typical pattern of EMB formation is shown in the inset of Fig. 1. The incident HCP is assumed to have the same profile as an EMB, but with an amplitude  $f_0$  and length  $\tau_0$  that are unrelated:

$$f(\tau) = f_0/\cosh(2\tau/\tau_0). \quad (4)$$

For a given  $\tau_0$ , a threshold (minimal) amplitude  $f_{\text{thr}} = 4/\tau_0$ , or  $E_{\text{thr}} = 2\hbar/t_0d$ , is required for attainment of a single EMB. In most of our runs we used  $\tau_0 = 4000$ , corresponding to  $t_0 \sim 313$  fs (or 413 fs at the pulse's half-amplitude), for Xe ( $\hbar\omega_0 \approx 8.5$  eV,  $d/e \approx 0.7$  nm) (Ref. 7 and 10); in this case  $f_{\text{thr}} = 10^{-3}$  and  $E_{\text{thr}} \approx 60$  kV/cm. The inset of Fig. 1 depicts a double-EMB formation for  $f_0 = 2f_{\text{thr}}$ ; the larger EMB is  $3f_{\text{thr}} = (3/2)f_0 \rightarrow 180$  kV/cm strong, and the weaker,  $f_{\text{thr}}$ ; they are 104 and 313 fs long, respectively. As  $f_0$  increases, more EMB's are formed, and the strongest EMB moves faster and leads the train; this precursor grows stronger and shorter, and the distance  $\zeta_{\text{EMB}}$  (Fig. 1), at which it breaks away, decreases. For a value of  $E_0 = 2$  MV/cm ( $f_0 \approx 3.3 \times 10^{-2} = 33f_{\text{thr}}$ ), expected to be achievable in the near future,<sup>11</sup>  $z_{\text{EMB}}$  is estimated [relation (10), below] as  $\zeta_{\text{EMB}} \sim 1.23 \times 10^5$ ; for Xe at 1 atm ( $Q \sim 5.7 \times 10^{-2}$ )  $\zeta_{\text{EMB}}$  translates into  $z_{\text{EMB}} \sim 10$  cm. The precursor here is 4.8 fs long, two orders of magnitude shorter than available HCP's.

In our computer simulations using HCP's with various profiles [in particular, Gaussian,  $f(\tau) \propto \exp[-(t/t_0)^2]$ , and  $\cosh^{-1}$  as in [Eq. (4)], we found that an EMB precursor shows a linear dependence of its amplitude  $f_{\text{EMB}}$  on the incident amplitude  $f_0$  (see Fig. 2):

$$f_{\text{EMB}} \approx af_0 - (a - 1)f_{\text{thr}}, \quad a = \text{constant} \sim 2. \quad (5)$$

With  $a = 2$ , Eq. (5) becomes exact for the profile [Eq. (4)]. Equation (5) also gives the precursor's length:  $\tau_{\text{EMB}} \approx \tau_{\text{thr}}/(2 - \tau_{\text{thr}}/\tau_0)$ , where  $\tau_{\text{thr}} = 4/f_0$ . The largest EMB becomes independent of the HCP's length  $\tau_0$  when  $\tau_0 \gg \tau_{\text{thr}}$  (inset of Fig. 2). Thus, to attain a strong and short EMB, one needs a strong, but not necessarily a short, HCP.

To explain these results and to find other characteristics of the EMB's, in particular their formation distance, we use an approach reminiscent of that developed in the theory of modulation instability in self-focusing and propagation of pulses in nonlinear optical fibers. Noting that an initially long and smooth HCP can be regarded as an almost-dc wave with the HCP's amplitude, and by readily evaluating the propagation characteristics of this wave, we analyze the behavior of its small perturbations. Linearizing the original equations with respect to these perturbations and deriving a dispersion equation for their spectral components, we then find the spectral component that has the fastest phase change. The characteristics of this

unique component will point to an EMB precursor that will develop out of it.

A field with  $f_0 = \text{constant}$  results in  $\eta_0 = \Omega_{\text{ST}}^{-1}$ ,  $p_0 = f_0\Omega_{\text{ST}}^{-1}$ ,  $QM_0 = \Omega_{\text{ST}}$ , and  $\beta_0 = (1 + Q\Omega_{\text{ST}}^{-1})^{-1/2}$ , where  $\Omega_{\text{ST}} \equiv (1 + f_0^2)^{1/2}$  is the Stark-shifted frequency of a TLS. Solving full Maxwell + Bloch equations (1) and (2) for small perturbations of this solution, and their spectral components,  $\exp[i(q\tilde{\zeta} - \Omega\tau)]$ , we obtain the dispersion relationship between  $q$  and  $\Omega$ :

$$q = \Omega \left[ 1 + Q/\Omega_{\text{ST}}(\Omega_{\text{ST}}^2 - \Omega^2) \right]^{1/2}. \quad (6)$$

In the low-frequency ( $\Omega \rightarrow 0$ ), linear limit we have  $q_{\text{LN}} = \Omega(1 + Q)^{1/2}$ . If  $Q \ll 1$ , the portion of  $q$  that is due to both the nonlinearity and dispersion is  $\Delta q = q - q_{\text{LN}} \approx Q\Omega/2[\Omega_{\text{ST}}(\Omega_{\text{ST}}^2 - \Omega^2)^{-1} - 1]$ . The lowest  $\Delta q(\Omega) < 0$  corresponds to the fastest perturbation. Looking for the minimum of  $\Delta q$ , we obtain the frequency,  $\Omega = \Omega_{\text{fast}}$ , of this component as

$$(\Omega_{\text{fast}}/\Omega_{\text{ST}})^2 = \left[ 2\Omega_{\text{ST}}^3 + 1 - (8\Omega_{\text{ST}}^3 + 1)^{1/2} \right] / 2\Omega_{\text{ST}}^3 \quad (7)$$

(if  $f_0^2 \ll 1$ ,  $\Omega_{\text{fast}} \approx f_0^2/2$ ). Substituting  $\Omega = \Omega_{\text{fast}}$  into Eq. (6), we evaluate the phase velocity,  $\beta_{\text{fast}} \equiv \Omega_{\text{fast}}/q_{\text{fast}}$ , of this component in the case  $Q \ll 1$  as

$$\beta_{\text{fast}} \approx 1 - Q / \left[ 1 + (8\Omega_{\text{ST}}^3 + 1)^{1/2} \right]. \quad (8)$$

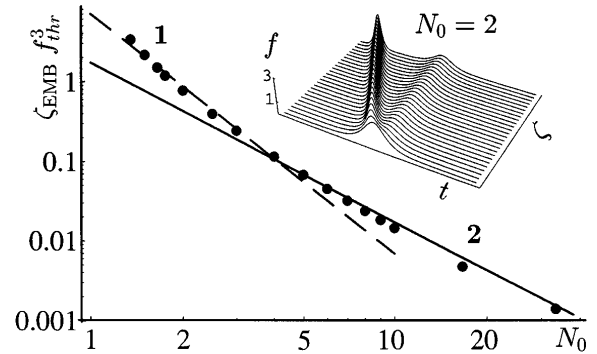


Fig. 1. Normalized formation distance  $\zeta_{\text{EMB}}f_{\text{thr}}^3$  of the EMB precursor versus normalized incident amplitude,  $N_0 = f_0/f_{\text{thr}}$ . Line 1,  $\pi\sqrt{5}/N_0^3$  [expression (9), below]; line 2,  $\sqrt{3}/N_0^2$  [expression (10), below]; filled circles, first saddle point appearance in a field profile. Inset, double-EMB formation by HCP with  $N_0 = 2$ .

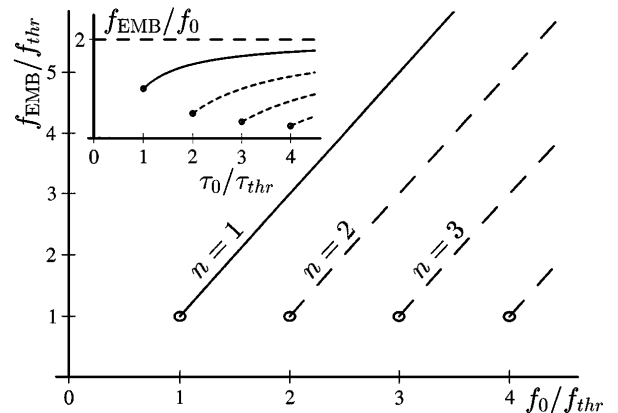


Fig. 2. EMB amplitude  $f_{\text{EMB}}$  versus the amplitude  $f_0$  and length  $\tau_0$  (inset) of the incident HCP. Solid curve, EMB precursor,  $n = 1$ ; broken curves, higher-order EMB's.

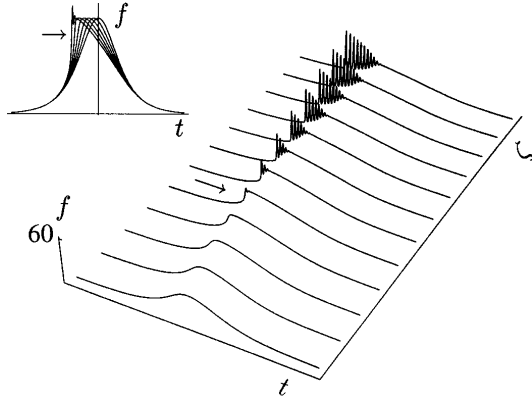


Fig. 3. Formation of a shocklike wave front for  $N_0 = 33$  as the wave propagates in  $\zeta$ . Inset, superimposition of the field profiles at different  $\zeta$ , illustrating the front formation.

Comparison with Eq. (3) shows that a matching EMB,  $\beta_{\text{EMB}} = \beta_{\text{fast}}$ , has an amplitude,  $f_{\text{fast}} = \{2[(8\Omega_{\text{ST}}^3 + 1)^{1/2} - 3]\}^{1/2}$ . For  $f_0^2 \ll 1$ , we have  $f_{\text{fast}} \approx 2f_0$ , which perfectly fits  $a = 2$  in Eq. (5). (In a dc field,  $\tau_0 \rightarrow \infty$  and thus  $f_{\text{thr}} \rightarrow 0$ , which explains the difference between Eq. (5) and  $f_{\text{fast}} = 2f_0$ .) To find the precursor formation distance  $\zeta_{\text{EMB}}$ , we use Eq. (6) with  $\Omega = \Omega_{\text{fast}}$  and estimate  $\zeta_{\text{EMB}}$  as  $\zeta$  at which a certain change of phase,  $\phi = 0(2\pi)$ , is accumulated (the best fit is provided by  $\phi = \pi\sqrt{10}$ ; see Fig. 1). If  $f_0^2 \ll 1$ ,  $\Delta q_{\text{fast}} \approx -Qf_0^3/\sqrt{2}$ , and  $\zeta_{\text{EMB}} \sim \pi\sqrt{10}/|\Delta q_{\text{fast}}| = 2\pi\sqrt{5}/Qf_0^3$  or

$$\zeta_{\text{EMB}} \sim \pi\sqrt{5}/f_0^3. \quad (9)$$

(curve 1 in Fig. 1). This compares well with the distance of the first appearance of a saddle point,  $\partial f/\partial\tau = \partial^2 f/\partial\tau^2 = 0$  (filled circles in Fig. 1), in the numerically obtained field profile up to  $(f_0/f_{\text{thr}})_{\text{cr}} = N_{\text{cr}} \sim 4$ . For larger  $f_0$ , when multiple EMB's are generated (see below), right before the EMB precursor breaks away, the initially smooth HCP drastically steepens to form a shocklike wave (Fig. 3), which unlike a dc ionization<sup>7</sup> shock wave can now appear far below ionization. Its formation distance  $\zeta_{\text{sh}}$  (line 2 in Fig. 1) is

$$\zeta_{\text{sh}} \approx \zeta_{\text{EMB}} \approx \sqrt{3}/f_0^2 f_{\text{thr}}, \quad f_0 > 4f_{\text{thr}}. \quad (10)$$

For profile (4), in the limit<sup>9</sup>  $f_0 \ll 1$ , the total number of EMB's,  $N_{\text{EMB}}$ , is

$$N_{\text{EMB}} = L(N_0), \quad N_0 \equiv f_0/f_{\text{thr}} = f_0\tau_0/4, \quad (11)$$

where  $L(x)$  is the largest integer that is not greater than  $x$ . For  $N_0 \gg 1$ ,  $N_{\text{EMB}} \approx N_0 = f_0\tau_0/4$ , i.e.,  $N_{\text{EMB}}$  is proportional to the incident HCP area. With the EMB precursor designated by the number 1, the amplitude  $f_n$  of the  $n$ th EMB is given as

$$f_n/f_{\text{thr}} = 2(N_0 - n) + 1, \quad n \leq N_0, \quad (12)$$

such that the decrement,  $f_{n-1} - f_n = 2f_{\text{thr}}$ , is independent of  $n$ , thus exhibiting quantum properties of EMB's. For the EMB precursor,  $n = 1$ , Eq. (12) coincides with Eq. (5), as expected. If  $f_0$  is an integer of  $f_{\text{thr}}$ , the incident HCP gives rise to an exact  $N$ -bubble solution. Otherwise, a part  $\Delta W_{\text{rad}}$  of its incident energy  $W_0$  is radiated away into nontrapped modes; their relative impact decreases rapidly as the total number of EMB's increases:  $\Delta W_{\text{rad}}/W_0 \leq N_0^{-2}$ .

In conclusion, we have found the characteristics of electromagnetic bubbles (their number, amplitudes, and lengths) formed by a half-cycle pulse of an arbitrary amplitude and length and estimated their formation distance. We demonstrated the formation of a shocklike front in a multibubble wave. Further research should include two- and three-dimensional propagation; in a transverse-limited EM field, a zero-frequency spectral component of the incident HCP will not propagate beyond the near-field area, and in the far-field area EMB will assume a modified profile.

This research is supported by the U.S. Air Force Office of Scientific Research. S. F. Straub was supported in part by the Deutsche Forschungsgemeinschaft. A. E. Kaplan (AEK) is a recipient of the Alexander von Humboldt Award of the AvH Foundation of Germany. AEK and P. L. Shkolnikov appreciate the kind hospitality of W. Schleich at Universität Ulm.

\*Also with Abteilung Für Quantenphysik, Universität Ulm, D-89091 Ulm, Germany.

## References

1. P. R. Smith, D. H. Auston, and M. S. Nuss, *IEEE J. Quantum Electron.* **24**, 255 (1988).
2. D. Grischkowsky, S. Keidin, M. van Exter, and Ch. Fattinger, *J. Opt. Soc. Am. B* **7**, 2006 (1990); R. A. Cheville and D. Grischkowsky, *Opt. Lett.* **20**, 1646 (1995).
3. J. H. Glowina, J. A. Misewich, and P. P. Sorokin, *J. Chem. Phys.* **92**, 3335 (1990).
4. B. B. Hu and M. S. Nuss, *Opt. Lett.* **20**, 1716 (1995).
5. R. R. Jones, D. You, and P. H. Bucksbaum, *Phys. Rev. Lett.* **70**, 1236 (1993); C. O. Reinhold, M. Melles, H. Shao, and J. Burgdorfer, *J. Phys. B* **26**, L659 (1993).
6. A. E. Kaplan, *Phys. Rev. Lett.* **73**, 1243 (1994); A. E. Kaplan and P. L. Shkolnikov, *J. Opt. Soc. Am. B* **13**, 412 (1996).
7. A. E. Kaplan and P. L. Shkolnikov, *Phys. Rev. Lett.* **75**, 2316 (1995); also in *Int. J. Non-Linear Opt. Phys. Mater.* **4**, 831 (1995).
8. R. K. Bullough and F. Ahmad, *Phys. Rev. Lett.* **27**, 330 (1971); J. E. Eilbeck, J. D. Gibbon, P. J. Caudrey, and R. K. Bullough, *J. Phys. A* **6**, 1337 (1973); E. M. Belenov, A. V. Nazarkin, and V. A. Ushchapovskii, *Sov. Phys. JETP* **73**, 423 (1991).
9. Propagation is more sensitive to the precision of constitutive equations than to that of Maxwell equations.<sup>7,8</sup> The former, however, can also be simplified within certain limits. For slow and weak fields ( $\tau_0^{-1}, f_0 \ll 1$ ), the Maxwell + constitutive equations can be reduced to a modified Kordeweg-De Vries equation for both the quantum and classical cases:  $\partial f/\partial\zeta - A_{\text{nl}}f^2\partial f/\partial\tau - \partial^3 f/\partial\tau^3 = 0$ , where for a TLS,  $A_{\text{nl}} = 3/2$ . In the opposite limit of a very strong and fast field, the Maxwell-Bloch equations can be reduced to a sine Gordon equation  $\partial^2\phi_R/\partial\zeta\partial\tau_1 = \sin\phi_R$  for a Rabi phase  $\phi_R \equiv \int_{-\infty}^{\tau_1} f d\tau$  ( $\tau_1 = \tau - \zeta$ ). Both of these equations are fully integrable and have single solitons of exactly the same profile as an EMB.
10. A. E. Kaplan and P. L. Shkolnikov, *Phys. Rev. A* **49**, 1275 (1994).
11. P. H. Bucksbaum, Department of Physics, University of Michigan, Ann Arbor, Mich. 48109 (personal communication, 1996).